Earthquake Engineering, Tenth World Conference © 1992 Balkema, Rotterdam. ISBN 90 5410 060 5

Dynamic uplift analysis of unanchored cylindrical tanks

D.T. Lau & X. Zeng
Department of Civil Engineering, Carleton University, Ottawa, Ont., Canada

R.W. Clough
University of California, Berkeley, Calif., USA

ABSTRACT: This paper presents an analysis procedure to study the dynamic uplift behavior of unanchored cylindrical tanks subjected to horizontal ground acceleration. The analysis procedure is based on a Ritz-type formulation with the fluid-tank system divided into substructure elements. The present formulation combines the advantage of the traditional Ritz method with some of the accuracy and convergence characteristics of the finite element formulation. Numerical results on the dynamic response of cylindrical tanks subjected to recorded earthquake ground motions are presented. Comparison of the seismic response behavior of anchored and unanchored tanks is also discussed.

1 INTRODUCTION

Cylindrical liquid storage tanks, particularly those that are unanchored, are very vulnerable to seismic damages. Studies of actual earthquake damages to liquid storage tanks have indicated that many of the tank damages were related to the uplift phenomenon. An unanchored tank uplifts significantly at the edge when subjected to horizontal base motion in response to the hydrodynamic loads generated by the vibrating fluid, as shown in Fig. 1. This dynamic uplift is a very complex nonlinear transient problem. Previous analytical studies on the dynamic behavior of cylindrical tanks have focused mainly on the response of anchored tanks (Haroun (1983), Veletsos and Yang (1977), Balendra et al. (1982), Ma et al. (1982), and Fischer (1979)), of which no separation of the tank shell base from the foundation is considered. Ishida and Kobayashi (1988) and Natsiavas and Babcock (1988) have modeled the rocking uplift response of unanchored tanks approximately by a nonlinear rotational spring.

This paper presents a time history analysis procedure to study the dynamic uplift behavior of unanchored cylindrical tanks subjected to horizontal line-break ground motion. The analysis procedure is based on a Ritz-type formulation of the fluid-tank system. Putting the analysis procedure in the finite element context, the uplifting cylindrical tank is divided into substructure elements, each formulated by the Ritz discretization. This analysis model can give the detailed displacement and stress time history response at any specified location in the fluid-tank system.

2 SYSTEM CONSIDERED

The system considered in the present study is a ground supported, flat bottom, open top, cylindrical steel tank of radius R and height H_s. The tank is partially filled with liquid to a depth of H_l. The bottom plate has a constant thickness of h_b. The cylindrical tank shell may have different course thicknesses, h_s, along the height. The liquid is assumed to be incompressible, inviscid, and free at the top surface. The fluid-tank system is described by a cylindrical coordinate system (r, θ, z), of which the origin is located at the center of the tank base. The longitudinal axis z is taken positive upwards.

The cylindrical tank is subjected to a horizontal translational component of ground shaking $\ddot{v}_g(t)$ along the axis $\theta = 0$.

3 STATIC TILT TEST AND ANALYSIS

Because of the complexity involved in dynamic uplift, the uplift mechanism has been studied experimentally under the simpler static tilt condition (Clough and Niwa (1979), Manos and Clough (1982), Sakai et al.(1988)), in which the rigid platform supporting the cylindrical tank is tilted up. Under this condition, an overturning moment generated from the hydrostatic pressure causes uplift of the tank bottom. The uplift

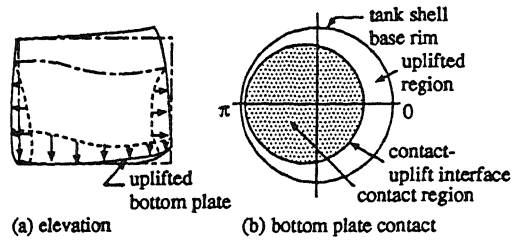

Figure 1. Uplift deformation under lateral loads

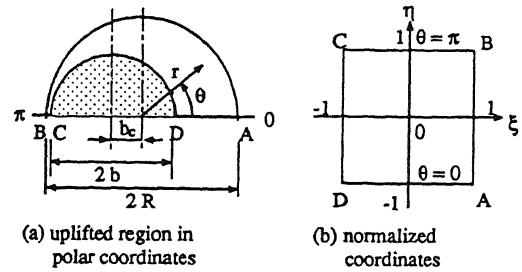

Figure 2. Coordinate mapping of uplifted region

mechanism involved in static tilt response is similar to that in dynamic uplift during earthquakes. Lau and Clough (1989) have studied the static tilt uplift behavior using derived Ritz shape functions. Analytical results from those studies indicate that the uplifted bottom plate has approximately a circular contact pattern, as shown in Fig. 1(b). Further studies by Lau and Zeng (1991) have developed an algorithm to define a simplified set of Ritz shape functions which are adapted here for nonlinear dynamic time history analysis.

4 RITZ FORMULATIONS

A dynamic analysis procedure is developed based on a Ritz-type approach. In the modeling of the flexible unanchored tank, the following basic assumptions are made:

1. The bottom plate uplifted region is modeled by the nonlinear von Karman plate theory in which the transverse flexural mechanism is coupled with the inplane membrane mechanism.
2. The uplifting cylindrical tank is assumed to remain elastic throughout the duration of the ground motion.
3. During dynamic response, the bottom plate contact boundary is assumed to have a circular shape.
4. The support foundation is assumed to be rigid, which implies that the transverse moment on the bottom plate along the contact-uplift interface is zero. This zero moment condition is the basis for the determination of the contact boundary position by iteration.
5. The lateral resultant force generated by the hydrodynamic pressure is resisted by friction distributed uniformly over the contact area.

4.1 *Ritz shape functions for bottom plate*

The Ritz displacement shape functions for the uplifted substructure element is presented here. Due to symmetry of the problem, it is sufficient to consider only half of the bottom plate in the analysis model. The crescent shape uplifted region shown in Fig. 2 is mapped into a curvilinear natural coordinate system (ξ, η) by linear mapping. In geometric coordinates, a natural coordinate line ξ, such as lines DA and CB in Fig. 2(a), varies along the radius of the bottom plate, whereas the lines η are evenly spaced between the inner contact-uplift interface and the outer base rim boundary. The η axes thus vary approximately in the tangential direction.

For convenience, the Ritz shape functions are defined in the natural coordinate system by separation of the two variables. A Ritz shape function has the general form of

$$N(\xi, \eta) = N_\xi(\xi) N_\eta(\eta) \tag{1}$$

where N_η gives the variation in the η direction, and N_ξ in the radial direction.

First, the Ritz shapes for the vertical displacement w are defined. Fig. 3(a) shows a typical variation of the vertical uplift displacement around the base rim obtained in a previous study on static tilt uplift. In contrast to Fourier analysis which involves many high order cosine terms, the function N_η^w in the present formulation consists of only two terms: a constant term and a $\cos\theta$ term modified by an offset parameter x_0 given as follows

$$N_\eta^w = \begin{cases} 1 \\ \cos\left[\frac{\pi}{2}(g(x_0, \eta) + 1)\right] \end{cases} \tag{2}$$

where $g(x_0, \eta) = \dfrac{x_0}{1 - x_0^2}(\eta^2 - 1) - \eta$

The modified cosine function together with the constant term can closely approximate the uplift displacement around the base rim, as shown in Fig. 3 by comparing the two curves. The magnitude of the offset depends on the amount of uplift, and thus the parameter x_0 is included as a degree of freedom in the analysis.

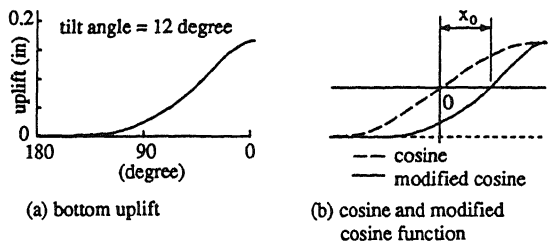

Figure 3. Modeling of displacement variation in tangential direction

For variation in the radial direction, the function N_ξ^w is given here by an infinite series of beam deflection shapes $\psi_1(\xi), \psi_2(\xi), \psi_3(\xi), \cdots$. The first five shapes in the series are shown in Fig. 4. As noted in the figure, the first two shapes are the boundary shapes, each having an unit displacement or rotation at the base rim ($\xi = 1$). The other shapes in the series are the interior shapes. Physically, these are the deflection shapes of a fixed-end beam subjected to transverse distributed loadings of increasing order.

Each combination of the above variations in ξ and η is an independent Ritz shape, the unknown magnitude of which is the Ritz coefficient. Higher accuracy of the solution can be obtained by using more Ritz shapes in the analysis. For the analysis procedure presented here, this may be interpreted as equivalent to reducing the element mesh size in finite element analysis.

The Ritz shape functions for the inplane displacement components, u_r and u_θ, can be obtained following a similar approach. The variations in the radial direction for the inplane shapes are shown in Fig. 5. Similar as before, the first two terms are the linear boundary shapes with unit displacement at one of the two ξ boundaries. The interior shapes are the deformations of an axially loaded bar. For the radial inplane displacement u_r, the normalized tangential variation N_η^r is the same as that of the vertical Ritz shapes given in Eq. (2). But for the tangential component u_θ, N_η^θ has only one term, which is the modified sine function obtained by replacing cosine with sine in Eq. (2).

In the modeling of the bottom plate, the behavior of the contact region substructure element can be obtained from analytical solution because of the simple geometry at its boundary. Displacement compatibility is maintained at the contact-uplift interface.

4.2 *Formulation of tank shell*

The cylindrical tank shell is modeled using Flügge linear thin shell theory (Flügge 1973). Exact analytical displacement shapes, compatible with those of

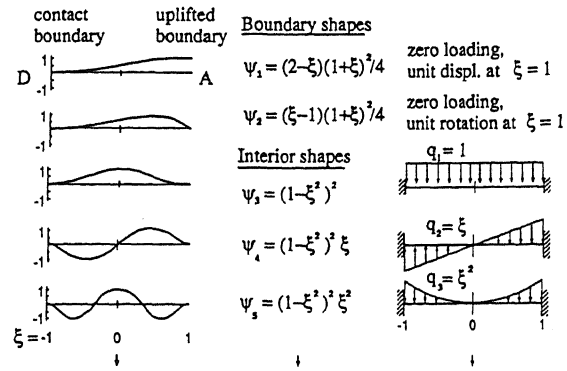

Figure 4. Function N_ξ for vertical Ritz shapes (uplifted region)

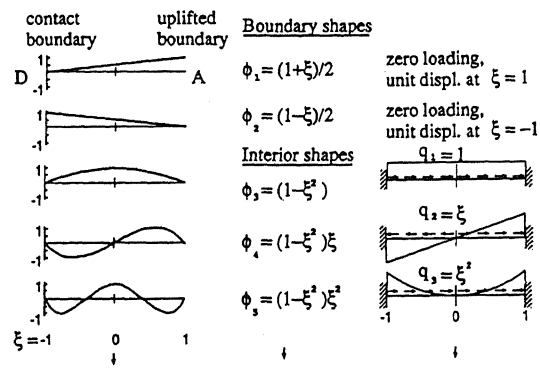

Figure 5. Function N_ξ for inplane Ritz shapes (uplifted region)

the bottom plate at the base rim connection, are derived. In order to minimize the number of degrees of freedom involved in nonlinear dynamic time history analysis, all the degrees of freedom at the top rim of the tank shell are statically condensed out, leaving only those at the base rim common with the bottom plate. The stiffening effects of the wind girder at the roof and other ring girders along the tank height are also considered in the formulation. Details of the tank shell formulation has been given by Lau and Clough (1989). This previous formulation has been extended to include varible tank shell thickness in the present study.

5 DYNAMIC EQUATION OF MOTION

Using the Ritz shape functions defined above and applying the virtual work principle, an equation of motion for the fluid-tank system can be obtained as follows

$$M\ddot{v} + C\dot{v} + Kv = p(t) - Mr\ddot{v}_g(t) \tag{3}$$

where v is the vector of the Ritz coefficients; M, C and K are the mass, damping, and stiffness matrices of the cylindrical tank respectively; $\ddot{v}_g(t)$ is the input horizontal ground acceleration; and r is the pseudostatic influence vector. The pressure loading vector $p(t)$ from the liquid is the sum of the hydrodynamic and hydrostatic pressure. For the hydrodynamic component, the effect of the tank shell flexibility and bottom plate uplift on the magnitude and distribution of the dynamic loading are considered. The hydrodynamic pressure is given as the sum of three separate components obtained by solving analytically a velocity potential Laplace's equation.

Since the uplift response of an unanchored tank is nonlinear, the equation of motion for the fluid-tank system is solved in the incremental form given as follows

$$M\Delta\ddot{v} + C\Delta\dot{v} + K\Delta v = \Delta p \tag{4}$$

where $\Delta p = (p_{d,n+1} - p_{d,n}) - Mr(\ddot{v}_{g,n+1} - \ddot{v}_{g,n})$

The symbol Δ denotes the increment of a response quantity from time t_n to t_{n+1}, and $p_{d,n}$ denotes the hydrodynamic loading vector at time t_n.

The hydrodynamic pressure acting on the tank surface depends on the deformation and uplift of the tank system, which are in turn modified by the hydrodynamic loading. Consequently, it can be shown that the term $(p_{d,n+1} - p_{d,n})$ is given in terms of $\ddot{v}$, which can then be modeled as added masses to the system. An effective mass matrix M_e can be obtained.

In nonlinear time history analysis, the incremental equation of motion given by Eq. (4) is typically solved by step-by-step integration. In the present formulation, the matrix incremental equation of motion for the MDOF fluid-tank system is first reduced to a generalized SDOF system by a generalized Ritz shape. The generalized Ritz shape Ψ employed is the deformation of the tank system obtained by applying the dynamic loads on the right hand side of Eq. (3) as static load on the tank system. Upon this reduction of degree of freedom, the generalized incremental equation of motion can be written as

$$\Delta\ddot{Y} + 2\omega^*\xi\Delta\dot{Y} + \omega^{*2}\Delta Y = \Delta P^* \; ; \quad v = \Psi Y \tag{5}$$

$$\begin{aligned} \text{where } \omega^{*2} &= (\Psi^T M_e \Psi)/(\Psi^T K \Psi) \\ \Delta P^* &= \Psi^T M r \Delta\ddot{v}_g \end{aligned}$$

In Eq. (5), Y is the generalized Ritz parameter, and ω^* is the pseudo natural circular frequency of the uplifting fluid-tank system.

6 TIME HISTORY ANALYSIS PROCEDURE

Due to the coupling of the hydrodynamic pressure with deformation of the tank system, the generalized Ritz shape obtained at the end of a time step, in general, will not correspond to the dynamic loading at that instant. Therefore an iterative procedure within each time step is necessary to obtain the proper generalized shape. The iterative time history analysis procedure consists of the following operations:

1. Starting with the converged results at the end of the previous time step t_n, determine the displacement, velocity and acceleration at the next time step t_{n+1}.
2. Determine the generalized Ritz shape Ψ_n at time t_n as the deformation due to dynamic loading at time t_n (Eq. 3) applied as static load.
3. Derive the generalized SDOF incremental equation of motion (Eq. 5) using Ψ_n. This incremental equation is then solved by time step integration using average acceleration method.
4. From the response at time t_{n+1} obtained in step 3, define an average acceleration as $\bar{\ddot{v}} = (\ddot{v}_n + \ddot{v}_{n+1}^{(i)})/2$.
5. Evaluate the dynamic loading corresponding to $\bar{\ddot{v}}$, which is then applied as a static load to obtain a new generalized Ritz shape $\bar{\Psi}_{n+1}^{(i)}$.
6. Check the convergence of the generalized Ritz shape for the current time step against a specified tolerance

$$\left| 1 - \frac{\bar{\Psi}_{n+1}^{(i)T} M \bar{\Psi}_{n+1}^{(i+1)}}{\bar{\Psi}_{n+1}^{(i+1)T} M \bar{\Psi}_{n+1}^{(i+1)}} \right| < \varepsilon \tag{6}$$

If the generalized Ritz shape has converged, go to step 1 and take $\Delta t = 0.1T^*$ as the time interval for the next time step. Otherwise, go back to step 3 and iterate until convergence.

7 NUMERICAL EXAMPLES

Numerical results of time history analyses of a broad 1/3 scale welded aluminum model tank, as shown in Fig. 6, are presented. This model tank had been tested on the shaking table at Berkeley by Manos and Clough (1982). The fluid-tank system is assumed to have a damping value 2% of the critical. The acceleration input is the north-south acceleration component recorded in the 1940 El Centro earthquake (Fig. 7).

For all three displacement components in the time history analysis, only the first three radial terms, two boundary and one interior shape, are included. The entire fluid-tank system is modeled by only 15 degrees of freedom in the present formulation. Higher accu-

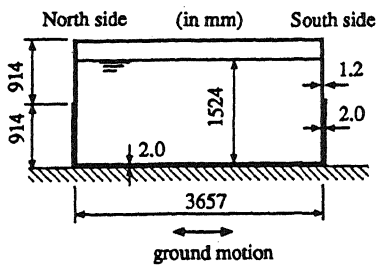

Figure 6. Configuration of an unanchored tank

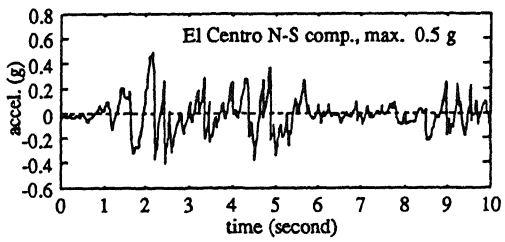

Figure 7. Earthquake acceleration input

racy can be obtained by including more Ritz shapes in the analysis, but this is found to be unnecessary.

First, dynamic response of the model tank under the unanchored support condition is presented. Figs. 8 and 9 show the time history of the lateral resultant force and overturning moment normalized by the total weight, $\bar{F}_0$ and $\bar{M}_0$, at the base of the vibrating system. Fig. 10 shows the time history of the base rim uplift at the excitation axis. As noted from the figure, the vertical uplift has a maximum about 5 times that of the plate thickness. This maximum uplift occurs not at the time of peak acceleration, bu at a later time when oscillation of the sloshing wave has built up, as evident in Figs. 8 and 9.

Time history of the axial membrane stress at a point on the cylindrical shell is given in Fig. 11. It is observed that the unanchored tank shell experiences spikes of high compressive axial stress on one side during uplift of the opposite side. The circumferential distribution of the tank shell axial membrane stress at a horizontal section near the base at the time of maximum is presented in Fig. 12. It is noted that the compressive stress is concentrated on the contact side of the excitation axis. The top rim out-of-round deformations at selected time intervals are plotted in Fig. 13.

For comparison, time history responses of the model tank under the anchored condition are also presented. The time histories of $\bar{F}_0$ and $\bar{M}_0$ shown in Figs. 14 and 15 for the anchored tank are similar to those of the unanchored case. As noted in Fig. 16, the anchored tank experiences smaller axial membrane stress, which is closely in phase with the overturning

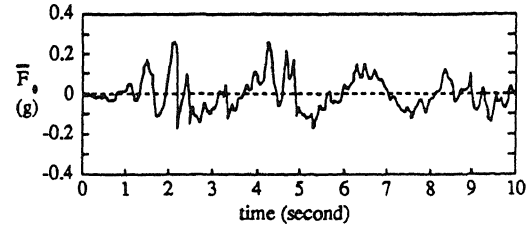

Figure 8. Normalized lateral resultant force of unanchored tank

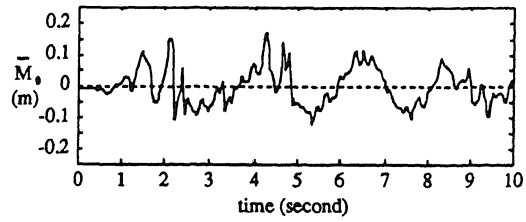

Figure 9. Normalized overturning moment of unanchored tank

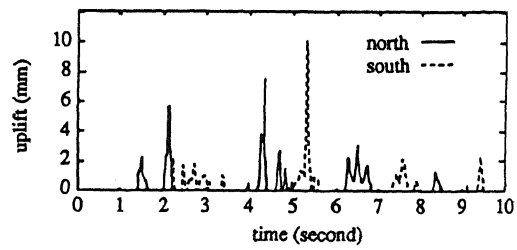

Figure 10. Uplift at excitation axis

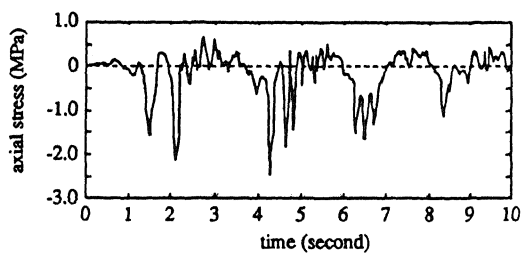

Figure 11. Axial stress of unanchored tank(25.4 mm above base)

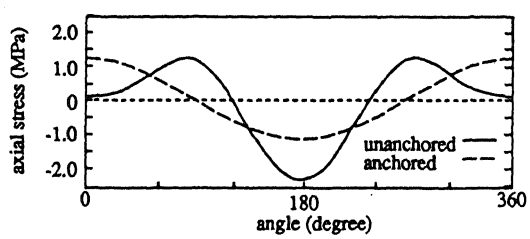

Figure12. Axial stress at horizontal section at 4.273 second

moment than a similar unanchored tank. There is no out-of-round deformation in any horizontal section. The $\cos\theta$ type circumferential distribution of axial membrane stress is plotted in Fig. 12.

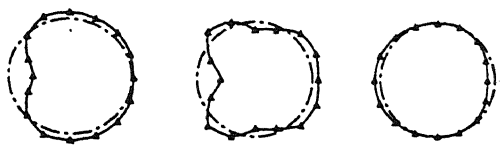

(a) at 2.194 s (b) at 4.695 s (c) at 5.158 s

Figure 13. Tank top rim out-of-round deformation (max. 9.5mm)

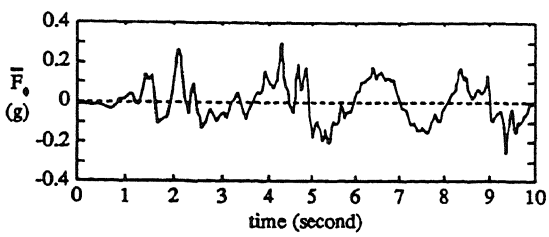

Figure 14. Normalized lateral resultant force of anchored tank

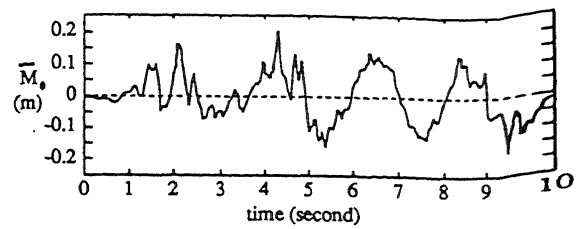

Figure 15. Normalized overturning moment of anchored tank

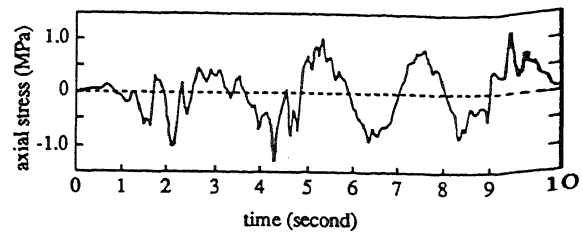

Figure 16. Axial stress of anchored tank

8 CONCLUSIONS

A time history analysis procedure has been developed to evaluate the nonlinear dynamic uplift response of unanchored cylindrical liquid storage tanks with flexible bottom. The analysis procedure is based on a substructuring approach, with each substructure element modeled by Ritz discretization. The efficiency of the procedure is demonstrated by the numerical example presented. Higher accuracy of the solution can be obtained by using more Ritz shapes from an infinite series in the analysis. Detailed displacement and stress time histories at any point in the fluid-tank system can be obtained. The analysis model may be employed to study the seismic performance of cylindrical tanks, particularly the dynamic buckling failures observed in many previous earthquakes, which may lead to improvement in seismic resistant design of these structures.

REFERENCES

Balendra, T., Ang, K.K., Paramasivam, P., and Lee, S.L. 1982. Seismic design of flexible cylindrical liquid storage tanks. *Earthquake Engineering and Structural Dynamics* 10:477-496.

Clough,R.W., Niwa,A. 1979. *Static tilt tests of a tall cylindrical liquid storage tank.* EERC-79/06, Earthquake Eng Res Center, Univ. of Calif. Berkeley.

Fischer, D. 1979. Dynamic fluid effects in liquid-filled flexible cylindrical tanks. *Earthquake Engineering and Structural Dynamics* 7:587-601.

Flügge, W. 1973. *Stresses in shells, 2nd ed.* Springer-Verlag, New York.

Haroun, M.A. 1983. Vibration studies and tests of liquid storage tanks. *Earthquake Engineering and Structural Dynamics* 11:179-206.

Ishida, K., and Kobayashi, N. 1988. An effective method of analyzing rocking motion for unanchored cylindrical tanks including uplift. *Transactions of the ASME* 110:76-87.

Lau,D.T., Clough,R.W. 1989. *Static tilt behavior of unanchored cylindrical tanks.* EERC-89/11, Earthquake Eng Res Center, Univ. of Calif., Berkeley.

Lau,D.T., and Zeng, X. 1991. Simplified uplift analysis of unanchored cylindrical tanks. *Proceedings of the Third U.S. Conference on Lifeline Earthquake Engineering*, Los Angeles, California:975-984.

Ma, D.C., Gvildys, J., Chang, Y.W., and Liu, W.K. 1982. Seismic behavior of liquid-filled shells. *Nuclear Engineering and Design* 70:437-455.

Manos,G.C., Clough,R.W. 1982. *Further study of the earthquake response of a broad cylindrical liquid-storage tank model.* EERC-82/07, Earthquake Eng Res Center, Univ. of Calif., Berkeley, CA.

Natsiavas, S., and Babcock, C.D. 1988. Behavior of unanchored fluid-filled tanks subjected to ground excitation. *Transactions of the ASME* 55:654-659.

Sakai, F., Isoe, A., Hirakawa, H., and Mentani, Y. 1988. Experimental study on uplifting behavior of flat-based liquid storage tanks without anchors. *Proceedings of Ninth World Conference on Earthquake Engineering*, Tokyo-Kyoto, Japan. VI:649-654.

Veletsos, A.S., Yang, J.Y. 1977. Earthquake response of liquid storage tanks. *Proceedings of Second Annual ASCE Engineering Mechanics Specialty Conference*, Raleigh, North Carolina: 1-24.